Published in final edited form as:
Brain Pathol. 2010 March ; 20(2): 343–350. doi:10.1111/j.1750-3639.2009.00283.x.

Alterations of Zinc Transporter Proteins ZnT-1, ZnT-4 and ZnT-6 in Preclinical Alzheimer's Disease Brain

Ganna Lyubartseva[1], **Jennifer. L. Smith**[1], **William R. Markesbery**[2,3], and **Mark. A. Lovell**[1,2,*]

[1]Department of Chemistry, University of Kentucky, Lexington, Kentucky

[2]Alzheimer's Disease Center, Sanders-Brown Center on Aging, University of Kentucky, Lexington, Kentucky

[3]Departments of Neurology and Pathology University of Kentucky, Lexington, Kentucky

Abstract

Our previous studies demonstrate alterations of zinc (Zn) transporter proteins ZnT-1, ZnT-4, and ZnT-6 in vulnerable brain regions of subjects with mild cognitive impairment (MCI), early and late stage Alzheimer's disease (AD) and suggest that disruptions of Zn homeostasis may play a role in the pathogenesis of AD. ZnT-1 exports Zn from the cytosol to extracellular compartments, ZnT-4 transports Zn from the cytosol to lysosomes and endosomes, and ZnT-6 sequesters Zn in the trans-Golgi network. A preclinical stage of AD (PCAD) has been described in which subjects show no overt clinical manifestations of AD but demonstrate significant AD pathology at autopsy. To determine if alterations of ZnT proteins occur in PCAD we measured ZnT-1, ZnT-4, and ZnT-6 in the hippocampus/parahippocampal gyrus (HPG) and cerebellum (CER) of 7 PCAD subjects and 7 age matched normal control (NC) subjects using Western blot analysis and immunohistochemistry. Our results show a significant decrease ($P < 0.05$) of ZnT-1 in HPG of PCAD subjects, along with an increase of ZnT-4 in PCAD CER and ZnT-6 in PCAD HPG, but a significant decrease in PCAD CER compared to NC subjects. Confocal microscopy of representative sections of HPG shows altered ZnTs are associated with neurons immunopositive for MC-1, a monoclonal antibody that identifies neurons early in formation of neurofibrillary tangles. Overall, our results suggest that alterations in Zn transport proteins may contribute to the pathology observed in PCAD subjects before onset of clinical symptoms.

Keywords

zinc transporter-1; zinc transporter-4; zinc transporter-6; preclinical Alzheimer's disease

INTRODUCTION

Alzheimer's disease (AD), the most common form of adult-onset dementia, currently affects 4.5 million Americans (22), and may affect 13.2 million by 2050, unless preventive strategies are found.

The major challenge associated with AD is that a definite diagnosis of AD is only possible at autopsy (42). Clinically, AD is characterized by progressive loss of memory and other cognitive functions (30). Neuropathologically, the AD brain is characterized by selective neuron and synapse loss, particularly in the hippocampus, amygdala, entorhinal cortex, and

*Correspondence to: Mark. A. Lovell, Sanders-Brown Center on Aging, 135 Sanders Brown Bldg., 800 S. Limestone St., Lexington, KY 40536. malove2@email.uky.edu..

nucleus basalis of Meynert; an abundance of neurofibrillary tangles (NFTs) containing hyperphosphorylated tau; and senile plaques composed of amyloid beta peptide (Aβ). Currently, the pathogenesis of AD remains unclear. With the recent characterization of subjects in prodromal and early stages of AD, there has been considerable research interest to identify changes in the brain of these subjects (23).

Although clinical manifestations of AD are age-dependent, increasing evidence suggests the initial neuropathological events that trigger AD may begin at an earlier age (17, 25). Data from neuropathological studies of 2,661 brains (age range from 25 to 95 years) show neurofibrillary alterations develop at around 40 years of age (5). Another study showed amyloid plaques in the neocortex distinguish early stages of AD from normal brain aging (34). In addition to the concept of amnesic mild cognitive impairment (MCI) as an early stage of AD with a high rate of progression to AD, a preclinical stage of AD (PCAD) has recently been proposed that is characterized by AD neuropathology in the absence of clinical manifestations and may precede the development of MCI and AD (17, 21, 24). Therefore, study of subjects with PCAD may provide insight into the pathogenesis of AD.

Numerous hypotheses have been proposed for AD etiology/pathogenesis including the oxidative stress hypothesis (30), the amyloid cascade hypothesis (41), and the trace element hypothesis (12) among others. In the present study we focused on the trace element hypothesis and the potential role of disruptions of zinc (Zn) homeostasis in the pathogenesis of AD. Zn, an essential trace element, functions as a regulatory factor for catalytical activity of numerous metalloenzymes. In addition, Zn stabilizes the conformation of Zn-dependent domains of transcriptional regulatory proteins (15). In brain, three classes of proteins regulate Zn at the cellular level: metallothioneins (MT), Zn transporters (ZnT), and members of ZIP family (zinc-regulated and iron-regulated transporter proteins) (11). Metallothioneins function to immediately coordinate intracellular Zn whereas Zn transporters mediate Zn efflux from cells or influx into intracellular vesicles. In contrast, ZIP proteins promote Zn transport from extracellular space or from intracellular vesicles to cytoplasm.

In general ZnTs have six transmembrane domains and histidine rich loops which connect these domains (35). Transcripts of four Zn transporters are present in mammalian brain: ZnT-1, ZnT-3, ZnT-4, and ZnT-6. ZnT-1 is located on the plasma membrane and is responsible for Zn export from the cytosol to the extracellular space during periods of elevated cytosolic Zn. This transporter is abundant in areas rich in synaptic Zn and has been proposed to have a protective role against Zn cytotoxicity in the nervous system (37). Our previous study of ZnT-1 showed a significant decrease in levels of ZnT-1 in MCI hippocampus/parahippocampal gyrus (HPG), but a significant elevation in early AD (EAD) and late AD (LAD) (28). ZnT-4 is located on lysosomal and endosomal compartments and functions to sequester Zn in these compartments. Our previous studies show elevated levels of ZnT-4 in HPG of EAD and LAD subjects (38). ZnT-6 sequesters Zn to the trans-Golgi network (TGN), and is increased in HPG of LAD and EAD subjects compared to NC subjects (38).

Most studies of preclinical cases have evaluated clinical parameters, whereas few studies have examined neuropathological changes that occur in PCAD (17). In the present study, we determined if there are alterations in ZnT-1, ZnT-4, and ZnT-6 in the brains of PCAD subjects.

MATERIALS AND METHODS

Brain Specimen Sampling

Tissue specimens from HPG and cerebellum (CER) of short postmortem interval (PMI) autopsies of seven PCAD and seven age matched normal control (NC) subjects were obtained through the neuropathology core of the University of Kentucky Alzheimer's Disease Center (UK-ADC). These samples were immediately frozen in liquid nitrogen and stored at –80°C until used for analysis.

PCAD and NC subjects were followed longitudinally in the UK-ADC Normal Control Clinic and had neuropsychologic testing, physical and neurological examinations annually. All NC subjects had neuropsychological test scores in the normal range and showed no evidence of memory decline. Although there are not precise criteria for the diagnosis of PCAD, the UK-ADC tentatively describes PCAD subjects as those with sufficient AD pathologic alterations to meet intermediate, or rarely, high NIA-Reagan Institute (NIA-RI) criteria with Braak scores of III-V, moderate or frequent neuritic plaque score according to Consortium to Establish a Registry for AD (CERAD), and antemortem psychometric test scores in the normal range when corrected for age and education. Recent studies by Galvin et al. (21) and Knopman et al. (24) reported that ~ 30% of control subjects had high or intermediate NIA-RI changes but were not demented and were likely PCAD subjects.

All subjects had neuropathological examination of multiple sections of neocortex, hippocampus, entorhinal cortex, amygdala, basal ganglia, nucleus basalis of Meynert, midbrain, pons, medulla, and CER using the modified Bielschowsky stain, hematoxylin and eosin stains, and Aβ and α-synuclein immunostains. Braak staging scores (4) were determined using the Gallyas stain on sections of entorhinal cortex, hippocampus, and amygdala and the Bielschowsky stain on neocortex. Histopathologic examination of NC subjects showed only age-associated changes and Braak staging scores of I to III. Four NC subjects did not meet CERAD criteria for histopathologic diagnosis of AD and two NC subjects met CERAD criteria for probable AD. All NC subjects met NIA-RI low likehood criteria for histopathologic diagnosis of AD. Three PCAD subjects did not meet CERAD criteria for the diagnosis of AD, three PCAD subjects met CERAD criteria for probable AD and two PCAD subjects had plaque pathology which corresponds to definite diagnosis of AD according to CERAD criteria. All PCAD subjects met intermediate or rarely high NIA-RI criteria (Braak III).

Tissue Processing

Tissue specimens were homogenized in 10 mM 2-[4-(2-hydroxyethyl)-1-piperazinyl]-ethanesulfonic acid (HEPES) containing 137 mM NaCl, 4.6 mM KCl, 0.6 mM MgSO4, 0.7 μg/ml pepstatin A, 0.5 μg/ml leupeptin, 0.5 μg/ml aprotinin, and 40 μg/ml phenylmethyl sulphonyl fluoride, using a Dounce homogenizer on ice. The resulting homogenate was centrifuged at 800x *g* and 4°C. The pellet was discarded and supernatant centrifuged at 100,000xg for 1 hr and 4°C. The supernatant was removed and used for ZnT-4 and ZnT-6 measurements. The pellet, used for ZnT-1 measurements later, was rinsed twice with HEPES buffer and resuspended in HEPES buffer. The final pellet was homogenized and protein concentrations were determined for the pellet and supernatant using the Pierce bicinchoninic acid (BCA) protein assay (Sigma, St. Louis, MO).

Antibodies and Reagents

Custom rabbit anti-ZnT-1, anti-ZnT-4 and anti-ZnT-6 polyclonal antibodies were prepared by Chemicon (Temecula, CA, USA). The ZnT-1 antibody was produced against KLH conjugated peptide (GTRPQVSHGKE), which corresponds to amino acids 448-458 of the

carboxyl terminus of rat ZnT-1 protein and shows significant homology to human ZnT-1. The peptides used in the production of the other two antibodies were unique to the sequence of each human protein: ZnT-4 (DSCDNCSKQPEILKQRKV) and ZnT-6 (QGLRTGFTYIPSR). Rabbit anti-GAPDH was used as a protein loading control (Santa Cruz, CA, USA). Horseradish peroxidase conjugated goat anti-rabbit secondary antibody was purchased from Amersham Biosciences (Piscataway, NJ).

Western Blot Analysis

Protein samples (20 μg) were separated by electrophoresis on 4-15% gradient sodium dodecyl sulfate polyacrylamide gels and transferred to nitrocellulose membranes. Membranes were blocked in 5% dry milk in Tris-buffered saline (TBS) containing 0.05% Tween 20 (TTBS) solution for 1 hr at room temperature. Primary antibodies were incubated overnight at 4°C. The dilutions of primary antibodies were 1:500 for ZnT-1, ZnT-6, and 1:1000 for ZnT-4. Membranes were washed with TTBS three times at room temperature and incubated in horseradish peroxidase conjugated goat anti-rabbit secondary antibody for 2 hr at room temperature and washed. Bands were visualized using enhanced chemiluminescence (Amersham Biosciences, Piscataway, NJ, USA) using manufacturer's instructions. After development, the membranes were stripped and reprobed for GAPDH (1:5000 dilution) as a protein loading control. Band intensities of ZnT-1, ZnT-4, and ZnT-6 proteins are quantified using Scion Image Analysis software (Scion, Frederick, MD, USA).

Confocal Microscopy and Quantitative Comparisons

Confocal microscopy and quantitative comparisons of ZnT-1 and ZnT-6 intensities in HPG of PCAD and NC subjects were performed as described previously (27). Briefly, 10 μm sections of paraffin-embedded HPG from PCAD and NC subjects were cut using a Shandon Finesse microtome (Thermo Electron, Waltham, MA), placed on Plus-slides and rehydrated through xylene, descending alcohols, and water. Sections were incubated for 10 minutes in a 0.75 mg/ml trypsin type II (Thermo Electron, Waltham, MA) solution prepared in 150 mM Tris HCl (pH 7.6) containing 3.3 mM $CaCl_2$ at 37°C. The sections were washed three times in phosphate buffered saline (PBS), allowed to air dry and then incubated in 50 mM ammonium chloride at room temperature for 30 minutes.

For confocal microscopy, sections were incubated overnight in a 1:100 dilution of ZnT-1 or ZnT-6 and a 1:100 dilution of MC-1, a conformation-dependent monoclonal antibody that recognizes distinct pathologic confirmations of tau observed only in AD brain and identifies early NFT formation (kindly provided by Dr. Peter Davies). All primary antibody solutions were prepared in TBS containing 1% fetal bovine serum (FBS) (Invitrogen, Carlsbad, CA). Following thorough rinsing in TBS, the sections were incubated 1 hour with a 1:1000 dilution of Alexa-488 conjugated anti-rabbit and Alexa-673 conjugated anti-mouse secondary antibodies (Molecular Probes, Eugene, OR) prepared in TBS containing1% FBS. After 5 rinses in TBS and distilled/deionized water, the sections were coverslipped using fluorescent anti-fade (Molecular Probes) and imaged using a Leica DM IRBE confocal microscope equipped with argon, krypton and HeNe lasers and a 40X oil objective. Confocal images were captured from a single z plane without optical sectioning. Fluorescent intensities for ZnT-1, ZnT-6 and MC-1 were quantified using Leica software (Leica Microsystems Heidelberg GmbH, Mannheim, Germany).

Statistical Analysis

For the Western blot analysis individual integrated band densities were averaged for NC subjects and the intensity of each NC and PCAD band was normalized to mean control levels for each individual gel. Normalized values were compared using a 2-tailed Student's *t*-test and the commercially available ABSTAT software (Anderson Bell, Arvada, CO, USA).

Results are presented as mean ± S.E.M (% NC) for ZnT-1, ZnT-4, or ZnT-6. Results of MC-1, ZnT-1 and ZnT-6 immunohistochemical studies are reported as mean ± S.E.M (% NC). Correlation analyses of ZnT-1, ZnT-6 and MC-1 immunostaining were performed using ABSTAT.

RESULTS

Subject demographic data are shown in Table 1. There were no significant differences between PCAD and NC subjects in age or PMI. Median Braak staging scores were significantly higher in PCAD subjects (IV) compared to NC subjects (I). Western blot analysis showed the presence of ZnT-1 by the appearance of a band at ~ 52 kDa. ZnT-4 was observed at approximately 48 kDa and ZnT-6 at 51 kDa. Previous studies show the antibodies were specific for the proteins of interest (27, 28, 38, 39).

Figures 1, 2, and 3 show levels of ZnT-1, ZnT-4 and ZnT-6 as mean ± S.E.M. (% of NC) in HPG and CER of PCAD and age matched NC subjects. Levels of ZnT-1 in HPG of PCAD subjects were significantly ($P< 0.05$) lower (62.3 ± 3.8%; n=7) compared to NC subjects (100 ± 8.2%; n=7) (Fig. 1B). ZnT-1 levels in CER were not significantly different between PCAD and NC subjects (Fig. 1C). Analysis of ZnT-4 showed a significant ($P< 0.05$) modest increase in PCAD subjects (116.4 ± 4.0%; n=7) compared to NC subjects (100.0 ± 4.1%; n=7) only in CER (Fig. 2C). ZnT-6 was significantly elevated ($P< 0.05$) in HPG of PCAD subjects (157.2 ± 12.0%; n=7) compared to NC subjects (100 ± 9.0%; n=7) (Fig. 3B). ZnT-6 was also significantly increased ($P< 0.05$) in CER of PCAD subjects (120.3 ± 7.0%; n=7) compared to NC subjects (100.0 ± 13.9%; n=7) (Fig. 3C).

To localize alterations in ZnT-1 and ZnT-6 to specific neuron populations, we performed confocal microscopy experiments and quantitative comparisons of ZnT-1 and ZnT-6 in HPG of PCAD and NC subjects. Representative confocal images of sections double labeled for MC-1 and ZnT-1 in NC and PCAD brain are shown in Figure 4. NC neurons showed minimal MC-1 immunoreactivity (Fig. 4A, green) and relatively high ZnT-1 (Fig. 4B, blue). In contrast, PCAD neurons (Figure 4D, green) showed pronounced MC-1 but limited ZnT-1 staining (Fig. 4E, blue). Figures 4C and 4F show merged images. Representative confocal images of sections double labeled for MC-1 and ZnT-6 in NC and PCAD brain are shown in Figure 5. NC neurons with minimal MC-1 immunoreactivity (Fig. 5A, green) also had low levels of ZnT-6 (Fig. 5B, blue). Figure 5C shows a merged image of MC-1 and ZnT-6 immunostaining in NC HPG neurons. Figure 5D shows PCAD neurons strongly MC-1 positive (green) also showed pronounced ZnT-6 immunostaining (Fig. 5E, blue). Figure 5F is an MC-1/ZnT-6 merged image of PCAD neurons. Figure 6 shows quantitative comparisons of MC-1, ZnT-1 and ZnT-6 immunostaining in PCAD and NC HPG. MC-1 immunostaining was significantly elevated ($P< 0.05$) in PCAD (142.3 ± 15.9%; n=5) compared to NC neurons (100.0 ± 8.1%; n=5). In contrast, HPG sections of PCAD brain showed a significant decrease ($P< 0.05$) in ZnT-1 immunostaining (39.5 ± 7.8%; n=5) compared to NC subjects (100.0 ± 8.7%; n=5). Immunoreactivity of ZnT-6 was significantly ($P< 0.05$) higher in PCAD (140.4 ± 13.5%; n=5) compared to NC neurons (100.0 ± 9.5%; n=5). Immunostaining results were comparable to Western Blot data. Correlation analyses showed a significant ($P< 0.05$) negative correlation (r = -0.67) between MC-1 and ZnT-1 immunostaining and a significant ($P< 0.05$) positive correlation (r = 0.71) between MC-1 and ZnT-6 immunoreactivity in PCAD neurons.

DISCUSSION

One etiologic hypothesis suggested for the pathogenesis of AD that has received considerable interest is the trace element hypothesis, particularly the role of Zn (12, 31). Zn

is the second most abundant trace element in the body after iron (18) and is involved at all levels of signal transduction in the mammalian cell (3). Critical cellular functions including cell growth, proliferation, differentiation, and programmed cell death involve Zn in ionic or protein-bound forms. In addition, Zn moderates the activity of at least 300 enzymes and transcription factors and plays an important role in DNA and RNA transcription and replication (39). There are three distinct pools of Zn in the brain: a protein bound pool, an ionic pool of free or loosely bound ions, and a vesicular pool that is released during neurotransmission (19). Chelatable Zn is present in the hippocampus, amygdala, and the visual, and somatosensory cortices (18). Zn concentrations in gray matter vary from 50 to 200 μM (16). During neurotransmission concentrations of Zn can reach values from around 0.5 μM at the basal level (1) to 300 μM in synaptic cleft (32).

Increasing evidence suggests that disruptions of Zn homeostasis are related to neurodegeneration in AD (9, 12, 18, 26, 31). Bulk analysis of Zn shows significant elevations of Zn in AD brain (16). Numerous studies have shown significant elevations of Zn in hippocampus, cerebral cortex and amygdala of AD subjects compared to normal controls (10, 13, 14). In addition, Zn was found to be abundant in senile plaques in amygdala of AD brain (26, 33). Recent studies by Religa et al. (36) found more than twofold increase of Zn in cortex of AD subjects compared to control subjects. An elevation of Zn levels was accompanied by increased levels of Aβ in the same brain specimens. It is interesting that alterations of Zn concentrations were found in the most vulnerable areas to AD pathology, such as hippocampus and amygdala (10, 13, 14).

The role of Zn in AD pathogenesis is controversial and is inferred from experimental models (20). The effect of Zn on protein/peptide alterations observed in AD has been extensively studied (40). Pathologically the AD brain is characterized by accumulation of Aβ that results from proteolytic cleavage of amyloid precursor protein (APP). APP mutations observed in familial AD surround the sites of cleavage by three secretases: α-secretase, β-secretase, and γ-secretases. Cleavage by α-secretase leads to the production of soluble APP, whereas cleavage by β-secretase and γ-secretase produces Aβ. Interestingly, Zn can bind to both human APP and Aβ (9). When Zn binds to APP, it may alter the ability of α-secretase to cleave APP and produce neurotrophic secreted APP (sAPP). It was also observed by Bush et al. (7, 8) that Zn induces the aggregation of Aβ at Zn concentration as low as 0.8 μM. Recent *in vivo* studies show Zn chelating agents significantly decrease deposition of amyloid plaques in mouse models of Aβ deposition and improve cognition in humans (12, 20). Numerous reports demonstrate that Zn can act as a potential mediator of neuronal degeneration (reviewed in 18). Additionally, loss of neurons in epilepsy, ischemia, and traumatic brain injury is characterized by elevations of neuronal Zn (20). In contrast, Zn at low concentrations has been shown to inhibit Aβ toxicity in cell cultures (29). Zn concentrations at the cellular level are tightly regulated by three families of Zn binding proteins: members of ZIP family, MTs, and ZnTs (11, 35).

The present data show a significant decrease of ZnT-1 in the HPG of PCAD subjects compared to controls. We observed the same trend for MCI subjects in our previous study of ZnT-1(28). Because the hippocampus is one of the most vulnerable regions in AD (42), diminished ZnT-1 may be one of the earliest manifestations of the disease because ZnT-1 regulates Zn efflux from the cytosol to the extracellular space (35). A decrease in ZnT-1 levels may lead to increased intracellular Zn in HPG of PCAD and MCI brain. In a previous study, concentrations of Zn at 300-600 μM cause extensive neuronal death in cortical cell culture after 15 minutes of exposure (20). It is possible that neurons cannot tolerate increased intracellular Zn during early stages of AD (PCAD and MCI), and therefore increase ZnT-1 production as the disease progresses (EAD, LAD) as a compensatory response. It is also possible that elevated ZnT-1 in LAD may lead to increased extracellular

Zn, which can interact with Aβ and contribute to Aβ aggregation. Positive correlations between levels of ZnT-1 and senile plaques and NFT in amygdala of AD brain supports this hypothesis (28). We would expect that decreased ZnT-1 and consequent elevation of intracellular Zn in HPG of PCAD brain could result in increased levels of ZnT-4 and ZnT-6, which function to sequester Zn into cellular compartments.

We observed significant changes in ZnT-4 levels only in CER. Brock et al. found that the distribution of APP and Aβ are restricted to specific cell layers in CER and hippocampus (6). This finding together with our results indicates that changes in ZnT-4 levels may have an effect on APP processing in PCAD CER. Previously, we reported increased levels of ZnT-4 in HPG of EAD and LAD brain, however, we did not observe significant alterations of ZnT-4 in MCI compared to controls (38). Because CER shows minimal pathology in AD (4), our observations of elevated ZnT-4 in PCAD CER are somewhat surprising. The relatively small number of subjects analyzed may explain our observations. Further study is needed to evaluate the possible role of ZnT-4 in PCAD.

The first study of ZnT-6 expression in AD brain demonstrated an increase of ZnT-6 in HPG of MCI, EAD, and LAD subjects compared with age matched NC subjects (38). Similarly, our current results indicate a significant elevation of ZnT-6 in HPG and CER of PCAD subjects compared to NC subjects. It is likely that diminished ZnT-1 leads to increased ZnT-6 levels in PCAD. ZnT-6 is localized in the TGN, a likely site for APP cleavage by the γ-secretase complex, and may promote Aβ formation (2). At the same time, Zn binds specifically to human APP, and Zn binding to amyloid precursor protein (APP) inhibits proteolysis by α-secretase and causes Aβ aggregation (8). This suggests increased levels of ZnT-6 and sequestration of Zn in the TGN may promote Aβ processing as well as affect normal sorting and trafficking of vital proteins and lipids in TGN. In our previous study (27), we found increased ZnT-6 in degenerating neurons and a trend toward significant correlation between levels of ZnT-6 and Braak scores, which is based on NFT pathology in AD brain. Our immunohistochemical studies support our Western Blot analyses. We found a significant ($P< 0.05$) decrease in the intensity of ZnT-1 immunostaining of PCAD neurons compared to that of NC. These results are comparable to the ZnT-1 protein level decrease we observed using Western Blot analysis. Our previous studies showed significantly increased immunoreactivity of ZnT-6 in MCI brain (27) with a positive correlation between MC-1 and ZnT-6 levels. Here we found a similar trend in PCAD compared to NC brain, suggesting similarities between PCAD and MCI. Our Western blot data show a significant increase of ZnT-6 levels in PCAD HPG compared to NC. Confocal microscopy shows comparable results with increased ZnT-6 staining associated with MC-1 positive PCAD neurons.

In summary, our data show significant changes in levels of two Zn transporters ZnT-1 and ZnT-6 in vulnerable regions of PCAD brain. Our results show a significant decrease of ZnT-1 and a significant elevation of ZnT-6 in HPG and correlate with our findings in MCI, suggesting similarity of Zn regulation patterns in PCAD and MCI. We speculate that PCAD and MCI may represent the same stage of AD that is characterized by similar levels of histopathology but different clinical manifestations. PCAD subjects are clinically normal, whereas MCI patients have memory decline. Morris and Price (34) suggested that PCAD subjects may have protective factors that prevent or slow the development of dementia. Understanding of these factors would provide insight into pathology of AD and maximize chances of AD prevention. Together with observations of elevated Zn levels in AD, our data indicate that Zn regulatory proteins may be key mediating factors in PCAD pathophysiology. Future studies on Zn transporters in PCAD should attempt to clarify the role of Zn homeostasis in the prodromal stage of the disease.

Acknowledgments

The authors thank Ms. Paula Thomason for editorial assistance and Ms. Sonya Anderson for subject demographic data.

Contact grant sponsor: NIH; Contact grant number: 5P01-AG05119; Contact grant number: P30-AG028383; Contact grant number: 1-RO1-AG16269; Contact grant sponsor: Abercrombie Foundation.

REFERENCES

1. Assaf SY, Chung SH. Release of endogenous Zn2+ from brain tissue during activity. Nature. 1984; 308(5961):734–6. [PubMed: 6717566]
2. Baulac S, LaVoie MJ, Kimberly WT, Strahle J, Wolfe MS, Selkoe DJ, Xia W. Functional gamma-secretase complex assembly in Golgi/trans-Golgi network: interactions among presenilin, nicastrin, Aph1, Pen-2, and gamma-secretase substrates. Neurobiol Dis. 2003; 14(2):194–204. [PubMed: 14572442]
3. Beyersmann D, Haase H. Functions of zinc in signaling, proliferation and differentiation of mammalian cells. Biometals. 2001; 14(3-4):331–41. [PubMed: 11831463]
4. Braak H, Braak E. Neuropathological stageing of Alzheimer-related changes. Acta Neuropathol (Berl). 1991; 82(4):239–59. [PubMed: 1759558]
5. Braak H, Braak E. Frequency of stages of Alzheimer-related lesions in different age categories. Neurobiol Aging. 1997; 18(4):351–7. [PubMed: 9330961]
6. Brock B, Basha R, DiPalma K, Anderson A, Harry GJ, Rice DC, Maloney B, Lahiri DK, Zawia NH. Co-localization and distribution of cerebral APP and SP1 and its relationship to amyloidogenesis. J Alzheimers Dis. 2008; 13(1):71–80. [PubMed: 18334759]
7. Bush AI, Multhaup G, Moir RD, Williamson TG, Small DH, Rumble B, Pollwein P, Beyreuther K, Masters CL. A novel zinc(II) binding site modulates the function of the beta A4 amyloid protein precursor of Alzheimer's disease. Journal Biol Chem. 1993; 268(22):16109–12. [PubMed: 8344894]
8. Bush AI, Pettingell WH, Multhaup G, d Paradis M, Vonsattel JP, Gusella JF, Beyreuther K, Masters CL, Tanzi RE. Rapid induction of Alzheimer A beta amyloid formation by zinc. Science. 1994; 265(5177):1464–7. [PubMed: 8073293]
9. Bush AI, Pettingell WH, Paradis MD, Tanzi R. Zinc and Alzheimer's disease. Science. 1995; 268:1921–3. [PubMed: 17797535]
10. Cornett CR, Markesbery WR, Ehmann WD. Imbalances of trace elements related to oxidative damage in Alzheimer's disease brain. Neurotoxicology. 1998; 19(3):339–45. [PubMed: 9621340]
11. Cousins RJ, Liuzzi JP, Lichten LA. Mammalian zinc transport, trafficking, and signals. The J Journal Biol Chem. 2006; 281(34):24085–9.
12. Cuajungco MP, Faget KY. Zinc takes the center stage: its paradoxical role in Alzheimer's disease. Brain Res Brain Res Rev. 2003; 41(1):44–56. [PubMed: 12505647]
13. Danscher G, Jensen KB, Frederickson CJ, Kemp K, Andreasen A, Juhl S, Stoltenberg M, Ravid R. Increased amount of zinc in the hippocampus and amygdala of Alzheimer's diseased brains: a proton-induced X-ray emission spectroscopic analysis of cryostat sections from autopsy material. J Neurosci Methods. 1997; 76(1):53–9. [PubMed: 9334939]
14. Deibel MA, Ehmann WD, Markesbery WR. Copper, iron, and zinc imbalances in severely degenerated brain regions in Alzheimer's disease: possible relation to oxidative stress. J Neurol Sci. 1996; 143(1-2):137–42. [PubMed: 8981312]
15. Dufner-Beattie J, Langmade SJ, Wang F, Eide D, Andrews GK. Structure, function, and regulation of a subfamily of mouse zinc transporter genes. Journal Biol Chem. 2003; 278(50):50142–50. [PubMed: 14525987]
16. Ehmann WD, Markesbery WR, Alauddin M, Hossain TI, Brubaker EH. Brain trace elements in Alzheimer's disease. Neurotoxicology. 1986; 7(1):195–206. [PubMed: 3714121]
17. Fagan AM, Csernansky CA, Morris JC, Holtzman DM. The search for antecedent biomarkers of Alzheimer's disease. J Alzheimers Dis. 2005; 8(4):347–58. [PubMed: 16556966]
18. Frazzini V, Rockabrand E, Mocchegiani E, Sensi SL. Oxidative stress and brain aging: is zinc the link? Biogerontology. 2006; 7(5-6):307–14. [PubMed: 17028932]

19. Frederickson CJ. Neurobiology of zinc and zinc-containing neurons. Int Rev Neurobiol. 1989; 31:145–238. [PubMed: 2689380]
20. Frederickson CJ, Koh JY, Bush AI. The neurobiology of zinc in health and disease. Nat Rev Neurosci. 2005; 6(6):449–62. [PubMed: 15891778]
21. Galvin JE, Powlishta KK, Wilkins K, McKeel DW Jr. Xiong C, Grant E, Storandt M, Morris JC. Predictors of preclinical Alzheimer disease and dementia: a clinicopathologic study. Arch Neurol. 2005; 62(5):758–65. [PubMed: 15883263]
22. Hebert LE, Scherr PA, Bienias JL, Bennett DA, Evans DA. Alzheimer disease in the US population: prevalence estimates using the 2000 census. Arch Neurol. 2003; 60(8):1119–22. [PubMed: 12925369]
23. Hodges JR. Alzheimer's centennial legacy: origins, landmarks and the current status of knowledge concerning cognitive aspects. Brain. 2006; 129(Pt 11):2811–22. [PubMed: 17071920]
24. Knopman DS, Parisi JE, Salviati A, Floriach-Robert M, Boeve BF, Ivnik RJ, Smith GE, Dickson DW, Johnson KA, Petersen LE, McDonald WC, Braak H, Petersen RC. Neuropathology of cognitively normal elderly. J Neuropathol Exp Neurol. 2003; 62(11):1087–95. [PubMed: 14656067]
25. Lange KL, Bondi MW, Salmon DP, Galasko D, Delis DC, Thomas RG, Thal LJ. Decline in verbal memory during preclinical Alzheimer's disease: examination of the effect of APOE genotype. J Int Neuropsychol Soc. 2002; 8(7):943–55. [PubMed: 12405546]
26. Lovell MA, Robertson JD, Teesdale WJ, Campbell JL, Markesbery WR. Copper, iron and zinc in Alzheimer's disease senile plaques. J Neurol Sci. 1998; 158(1):47–52. [PubMed: 9667777]
27. Lovell MA, Smith JL, Markesbery WR. Elevated zinc transporter-6 in mild cognitive impairment, Alzheimer disease, and pick disease. J Neuropathol Exp Neurol. 2006; 65(5):489–98. [PubMed: 16772872]
28. Lovell MA, Smith JL, Xiong S, Markesbery WR. Alterations in zinc transporter protein-1 (ZnT-1) in the brain of subjects with mild cognitive impairment, early, and late-stage Alzheimer's disease. Neurotox Res. 2005; 7(4):265–71. [PubMed: 16179263]
29. Lovell MA, Xie C, Markesbery WR. Protection against amyloid beta peptide toxicity by zinc. Brain Res. 1999; 823(1-2):88–95. [PubMed: 10095015]
30. Markesbery WR. Oxidative stress hypothesis in Alzheimer's disease. Free Radic Biol Med. 1997; 23(1):134–47. [PubMed: 9165306]
31. Markesbery, WR.; Ehmann, WD. Trace element alterations in Alzheimer's disease.. In: Terry, RD.; Katzman, R., editors. Alzheimer's disease. Raven Press; New York: 1994.
32. Maynard CJ, Bush AI, Masters CL, Cappai R, Li QX. Metals and amyloid-beta in Alzheimer's disease. Int J Exp Pathol. 2005; 86(3):147–59. [PubMed: 15910549]
33. Miller LM, Wang Q, Telivala TP, Smith RJ, Lanzirotti A, Miklossy J. Synchrotron-based infrared and X-ray imaging shows focalized accumulation of Cu and Zn co-localized with beta-amyloid deposits in Alzheimer's disease. J Struct Biol. 2006; 155(1):30–7. [PubMed: 16325427]
34. Morris JC, Price AL. Pathologic correlates of nondemented aging, mild cognitive impairment, and early-stage Alzheimer's disease. J Mol Neurosci. 2001; 17(2):101–18. [PubMed: 11816784]
35. Palmiter RD, Huang L. Efflux and compartmentalization of zinc by members of the SLC30 family of solute carriers. Pflugers Arch. 2004; 447(5):744–51. [PubMed: 12748859]
36. Religa D, Strozyk D, Cherny RA, Volitakis I, Haroutunian V, Winblad B, Naslund J, Bush AI. Elevated cortical zinc in Alzheimer disease. Neurology. 2006; 67(1):69–75. [PubMed: 16832080]
37. Sekler I, Moran A, Hershfinkel M, Dori A, Margulis A, Birenzweig N, Nitzan Y, Silverman WF. Distribution of the zinc transporter ZnT-1 in comparison with chelatable zinc in the mouse brain. J Comp Neurol. 2002; 447(3):201–9. [PubMed: 11984815]
38. Smith JL, Xiong S, Markesbery WR, Lovell MA. Altered expression of zinc transporters-4 and -6 in mild cognitive impairment, early and late Alzheimer's disease brain. Neuroscience. 2006; 140(3):879–88. [PubMed: 16580781]
39. Vallee BL, Falchuk KH. The biochemical basis of zinc physiology. Physiol Rev. 1993; 73(1):79–118. [PubMed: 8419966]
40. Wilquet V, De Strooper B. Amyloid-beta precursor protein processing in neurodegeneration. Curr Opin Neurobiol. 2004; 14(5):582–8. [PubMed: 15464891]

41. Xie Z, Tanzi RE. Alzheimer's disease and post-operative cognitive dysfunction. Exp Gerontol. 2006; 41(4):346–59. [PubMed: 16564662]

42. Yaari R, Corey-Bloom J. Alzheimer's disease. Semin Neurol. 2007; 27(1):32–41. [PubMed: 17226739]

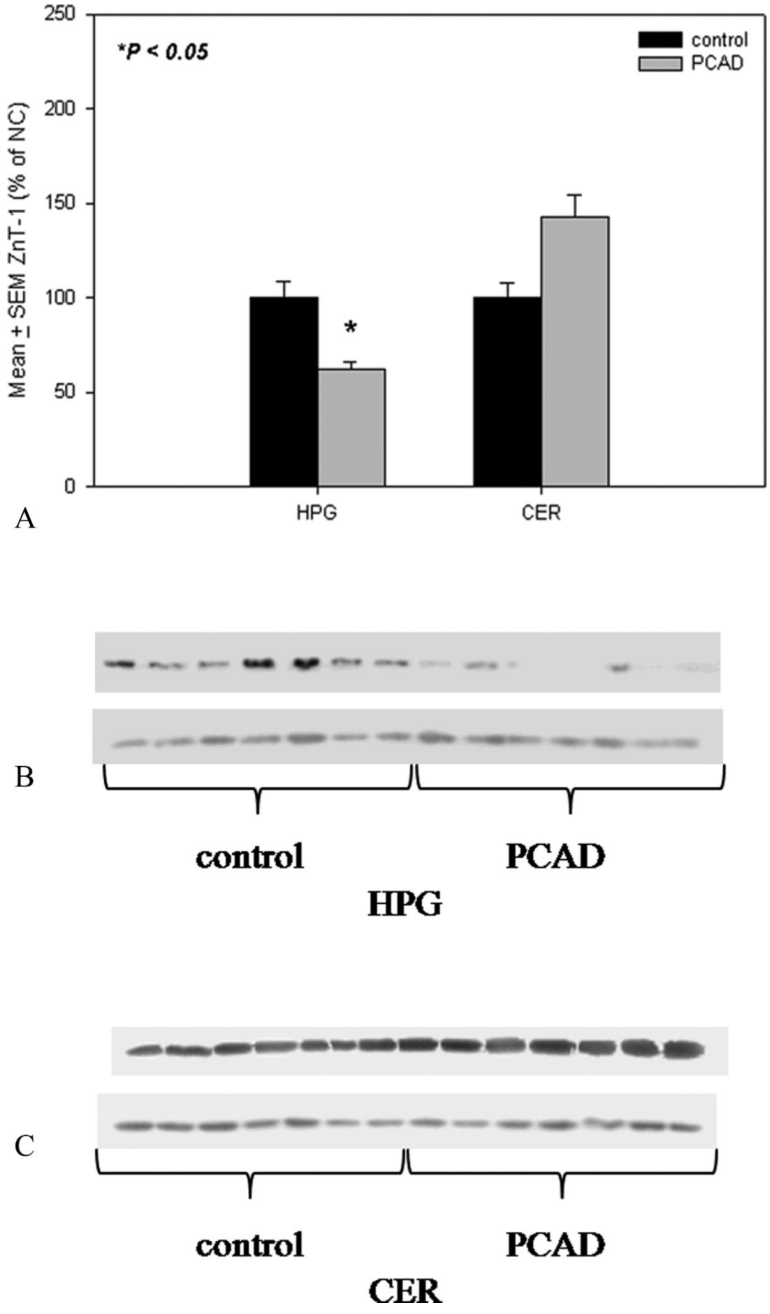

Fig.1.

ZnT-1 protein levels expressed as mean ± S.E.M. (% of NC) in HPG and CER of PCAD and NC subjects (**A**). ZnT-1 was significantly decreased ($P < 0.05$) in PCAD HPG compared to age matched NC subjects. Representative Western Blots of ZnT-1 (upper bands) and loading control GAPDH (lower bands) in HPG of PCAD and NC subjects (**B**). Representative Western Blots of ZnT-1 (upper bands) and loading control GAPDH (lower bands) in CER of PCAD and NC subjects (**C**).

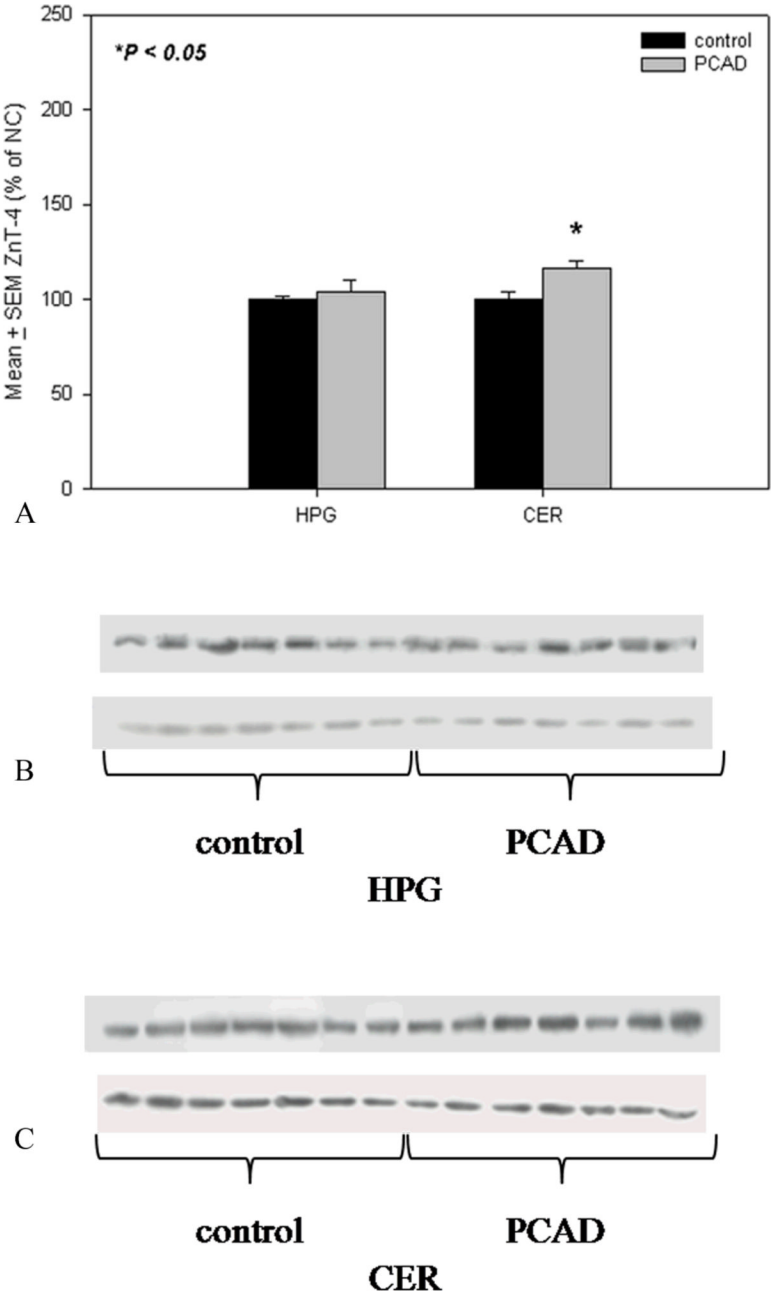

Fig.2.

ZnT-4 protein levels expressed as mean ± S.E.M. (% of NC) in HPG and CER of PCAD and NC subjects with loading control (GAPDH) underneath each blot (**A**). ZnT-4 was significantly increased ($P < 0.05$) in PCAD CER compared to age matched NC subjects. Representative Western Blots of ZnT-4 (upper bands) and loading control GAPDH (lower bands) in HPG of PCAD and NC subjects (**B**). Representative Western Blots of ZnT-4 (upper bands) and loading control GAPDH (lower bands) in CER of PCAD and NC subjects (**C**).

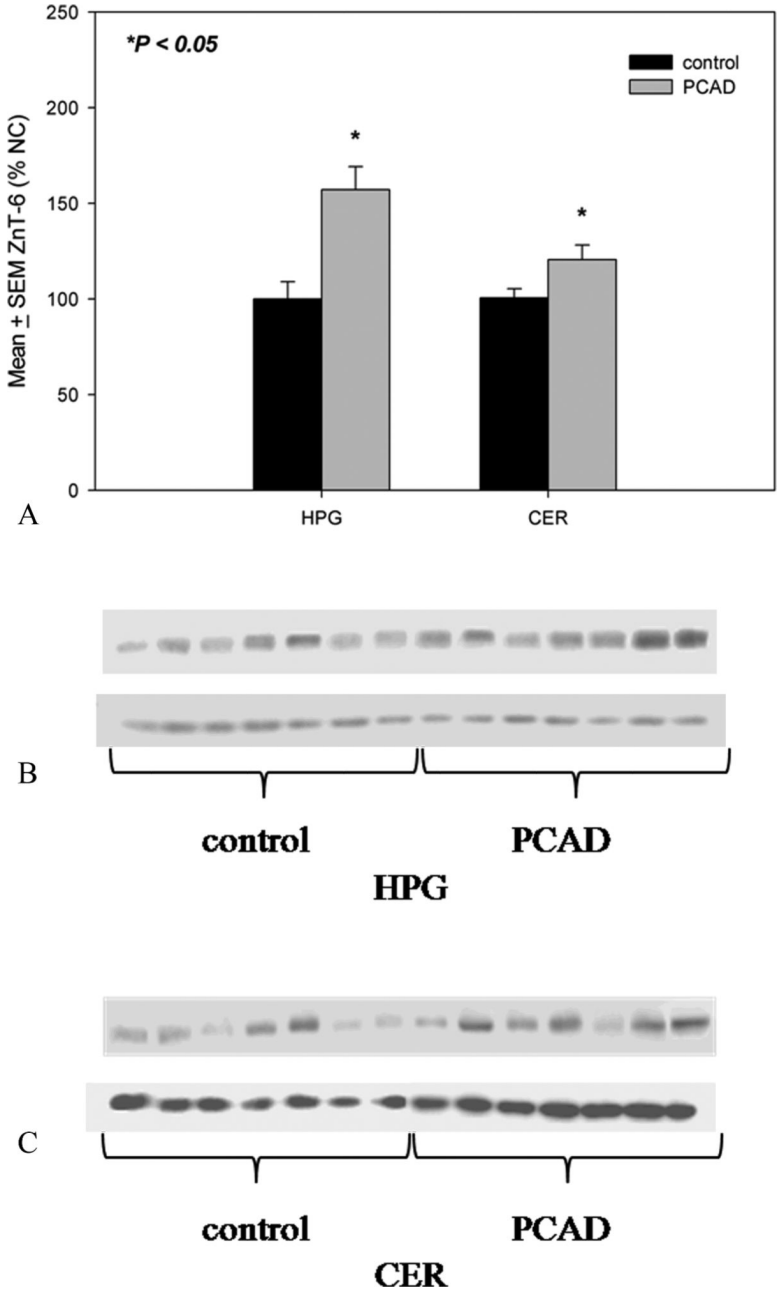

Fig.3.

ZnT-6 protein levels expressed as mean ± S.E.M. (% of NC) in HPG and CER of PCAD and NC subjects with loading control (GAPDH) underneath each blot (**A**). ZnT-6 was significantly increased ($P < 0.05$) in PCAD HPG and CER compared to age matched NC subjects. Representative Western Blots of ZnT-6 (upper bands) and loading control GAPDH (lower bands) in HPG of PCAD and NC subjects (**B**). Representative Western Blots of ZnT-6 (upper bands) and loading control GAPDH (lower bands) in CER of PCAD and NC subjects (**C**).

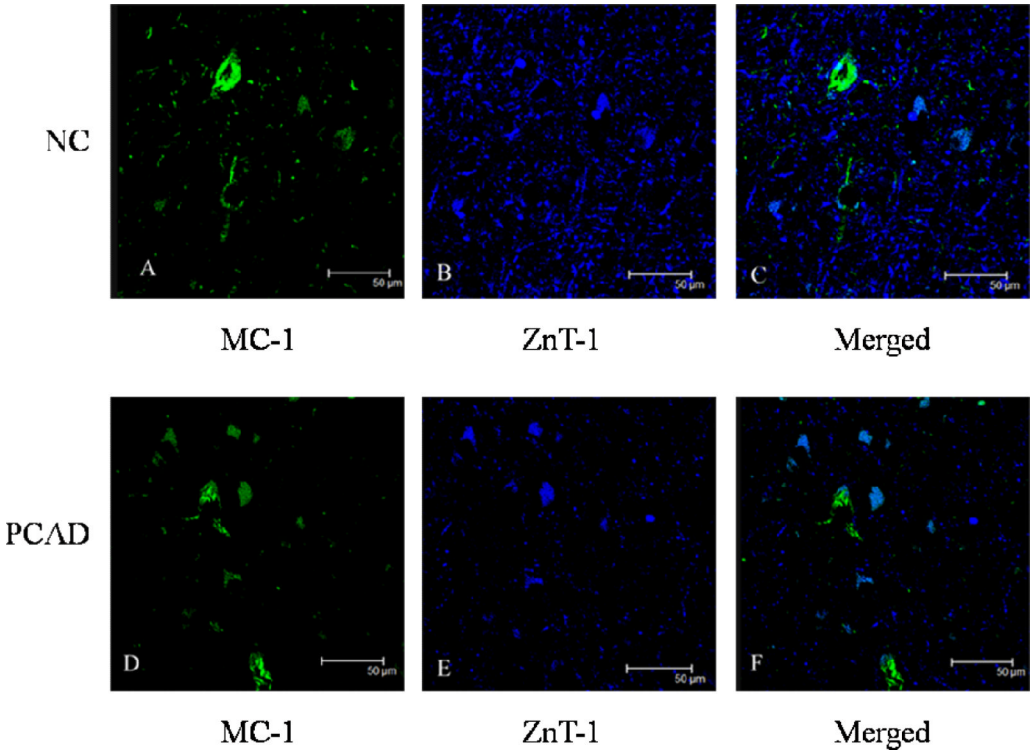

Fig.4.

Representative confocal micrographs of NC and PCAD HPG double labeled for MC-1 (green) and ZnT-1 (blue). NC: MC-1 (**A**), ZnT-1 (**B**) and a merged image (**C**). PCAD: MC-1 (**D**), ZnT-1 (**E**) and a merged image (**F**). Note NC neurons with minimal MC-1 and relatively high ZnT-1 staining in contrast to PCAD neurons with more pronounced MC-1 and less pronounced ZnT-1 immunostaining. Scale bar = 50 μm.

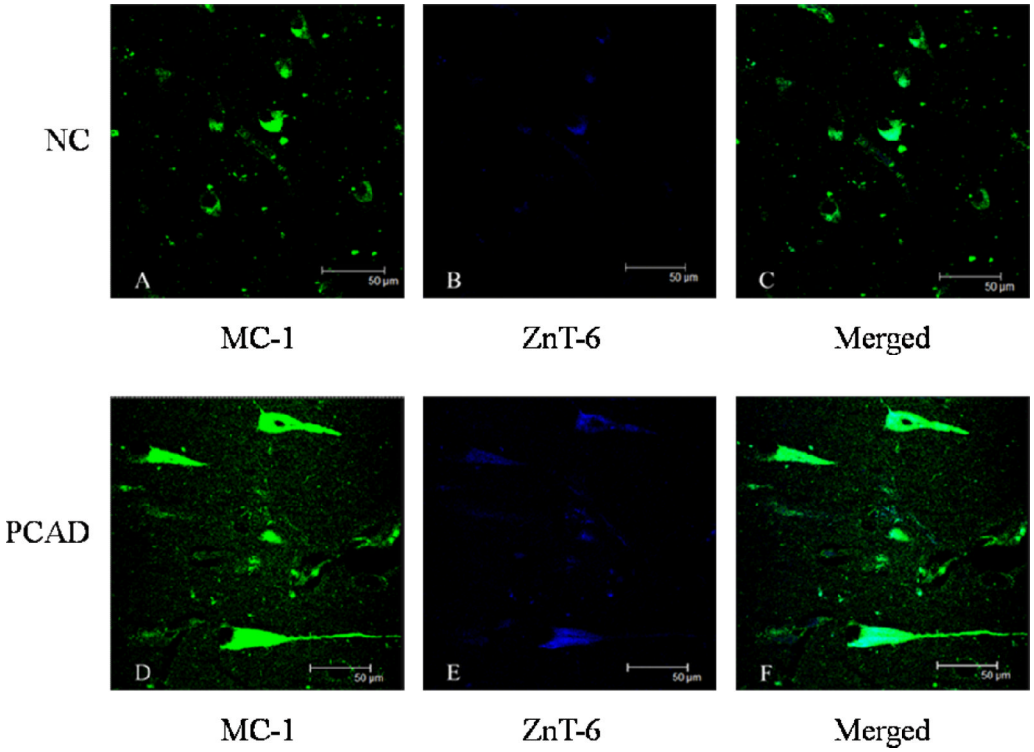

Fig.5.

Representative confocal microscopy of neurons from NC and PCAD HPG double labeled for MC-1 (green) and ZnT-6 (blue). NC: MC-1 (**A**), ZnT-6 (**B**) and a merged image (**C**). PCAD: MC-1 (**D**), ZnT-6 (**E**) and a merged image (**F**). Note NC neurons with minimal MC-1 and ZnT-6 staining in contrast to PCAD neurons with more pronounced MC-1 and ZnT-6 immunostaining. Scale bar = 50 μm.

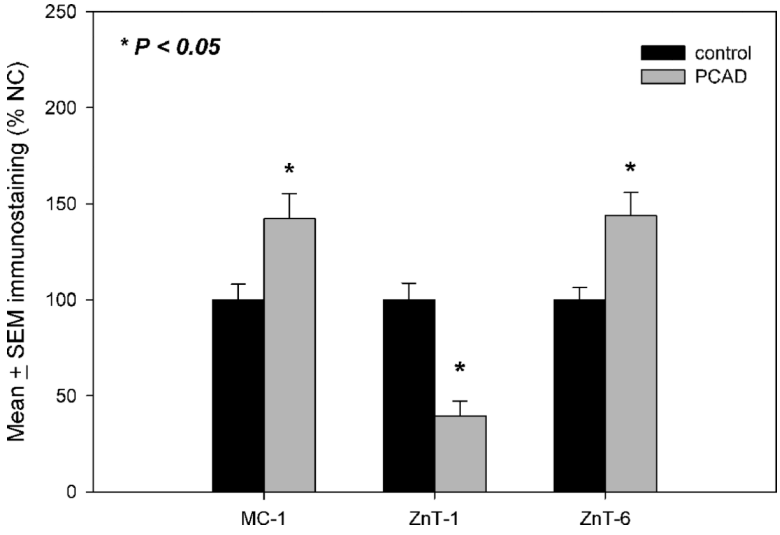

Fig.6.

Quantitative comparisons of MC-1, ZnT-1 and ZnT-6 immunostaining in PCAD and NC HPG brain sections. MC-1 and ZnT-6 was significantly increased and ZnT-1 was significantly decreased in PCAD ($P < 0.05$) compared to age matched NC subjects.

Table 1

Subject demographic data

Group	Mean ± SEM Age (y)	Sex	Mean ± SEM PMI (h)	Median Braak score
NC	86.7 ± 2.6	N=7; 2M, 5F	2.8 ± 0.24	I
PCAD	84.6 ± 1.9	N=7; 3M, 4F	2.9 ± 0.28	IV*

*$P < 0.05$